A Novel Exploration of the Choroidal Vortex Vein System: Incidence and Characteristics of Posterior Vortex Veins in Healthy Eyes

Guiqin He, Xiongze Zhang, Xuenan Zhuang, Yunkao Zeng, Yuhong Gan, Yongyue Su, Miaoling Li, Yuying Ji, Lan Mi, Xuelin Chen, and Feng Wen (ORCID)

State Key Laboratory of Ophthalmology, Zhongshan Ophthalmic Center, Sun Yat-Sen University, Guangdong Provincial Key Laboratory of Ophthalmology and Visual Science, Guangdong Provincial Clinical Research Center for Ocular Diseases, Guangzhou, China

PURPOSE. The purpose of this study was to investigate the incidence and characteristics of posterior vortex veins (PVVs) in healthy eyes and explore their relationship with age and refractive status.

METHODS. This retrospective cross-sectional analysis encompassed 510 eyes from 255 consecutive healthy participants. Wide-field optical coherence tomography angiography (WF-OCTA) imaging was used to assess the presence of PVVs. Eyes were classified according to refractive status (emmetropia, low and moderate myopia, and high myopia) and age (minors and adults). The incidence and characteristics of eyes with PVVs were analyzed.

RESULTS. Participants (mean age = 30.60 ± 21.12 years, 47.4% men) showed a mean refractive error of -2.83 ± 3.10 diopters (D; range = -12.00 to $+0.75$). PVVs were observed in 16.1% (82/510) of eyes. Of these, 39% (32/82) had PVVs in one eye and 61% (50/82) in both eyes. The mean number of PVVs per eye was 1.65 ± 1.05 (range = 1–6). PVVs are mainly around the optic disc (78%, 64/82) of eyes with PVVs and less in the macular area (6.1%, 5/82) or elsewhere (15.9%, 13/82). PVV incidence correlated with refractive status: 10.3% (22/213) in emmetropia, 16.6% (31/187) in low and moderate myopia, and 26.4% (29/110) in high myopia ($P = 0.001$), but not with age. Refractive status was the key predictor of PVV occurrence (odds ratio [OR] = 1.45, 95% confidence interval [CI] = 1.02–2.06, $P = 0.038$).

CONCLUSIONS. This study confirms PVVs' presence in healthy eyes, highlighting their inherent existence and susceptibility to alterations due to refractive conditions. These findings enhance our understanding of the vortex vein system and its distribution within the eyes.

Keywords: posterior vortex vein (PVV), healthy eyes, incidence, wide-field optical coherence tomography angiography (WF-OCTA), choroid, anatomy

The choroidal vascular system, as the largest and most significant vascular system in the eyes, plays a crucial role in supplying blood to both the outer retina and the anterior segment of the eyes.[1,2] The convergence of various veins from the choroidal vascular bed form several vortex veins, which exit the eyes through a scleral canal. The vortex vein system plays a crucial role in draining the high blood flow from the choroidal circulation, serving as an important pathway for choroidal drainage. This system can be anatomically partitioned into three primary sections: intraocular, scleral, and extraocular.[3] Within the eyes, numerous choroidal veins converge into an enlarged vestibule region known as the ampulla before penetrating the sclera and exiting the eyes.

Previous studies have reported the presence of multiple vortex veins exiting through the sclera, with the number of identified veins varying: 5 to 13 vortex veins were identified in 36 healthy eyes using ultra-widefield indocyanine green angiography (UWF-ICGA),[4] whereas 3 to 8 vortex veins were confirmed in the scleral exits of 46 autopsy eyes via a dissecting microscope.[5] Although the incidence of vortex veins showed variability, these exits are located at the eye's equator, serving as important landmarks.[6]

Occasionally, anomalous vortex veins exits can be located at the posterior pole of the eyes, associated with various chorioretinal diseases.[7–10] Several cases of vortex vein exits located at the macular area have been reported in individuals with high myopia.[11–13] Moriyama et al. identified posterior vortex veins (PVVs) in 11% highly myopic eyes using indocyanine green angiography (ICGA).[14] Recently, using UWF-ICGA, the same group found the frequency of PPVs in highly myopic eyes to be higher, around 26%.[15] However, it remains uncertain whether the existence of PVVs indicates an abnormal condition. Furthermore, it is unclear whether PVVs are congenital or acquired.[15] So far, there have been no reports on the distribution of PVVs in healthy eyes, much less their relationship with age and refractive status.

Investigative Ophthalmology & Visual Science
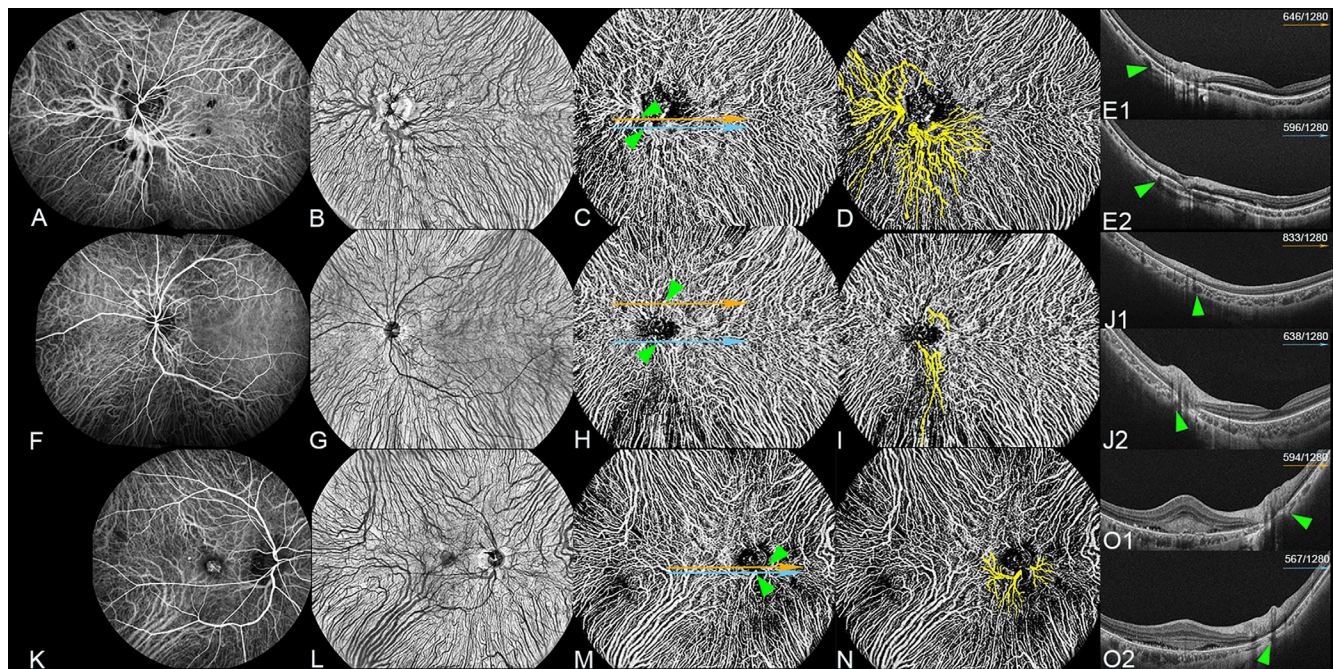
FIGURE 1. Comparison of PVV detection using ICGA venous phase and en face WF-OCTA (Subjects not included). (**A–E2**) Two PVVs located around the optic disc in an eye with punctate inner choroidopathy. (**A**) Detection of two PVVs around the optic disc using the ICGA venous phase. (**B**) Detection of two PVVs around the optic disc using 24×20 mm en face WF-OCTA in the large-vessel choroidal layer. (**C**) WF-OCTA image showing the large-vessel choroidal layer in the same scan as **B**, with two horizontal lines (*orange* and *blue arrows*) crossing the exit points of PVVs (*green arrowheads*). (**D**) The *yellow highlight* indicates the presence of two PVVs around the optic disc in **C**. (**E1**) Horizontal WF-OCT image of **C** (*orange arrow*) corresponds to the 646th scan out of a total of 1280 WF-OCT scans, clearly demonstrating the exit of one PVV penetrating the sclera (*green arrowhead*) and leaving the eyeball. (**E2**) Horizontal WF-OCT image of **C** (*blue arrow*) corresponds to the 596th scan out of a total of 1280 WF-OCT scans, clearly illustrating the exit of another PVV penetrating the sclera (*green arrowhead*) and leaving the eyeball. (**F–J2**) Two PVVs located around the optic disc in an eye with acute zonal occult outer retinopathy. (**F**) Detection of two PVVs around the optic disc using the ICGA venous phase. (**G**) Detection of two PVVs around the optic disc using 24×20 mm en face WF-OCTA in the large-vessel choroidal layer. (**H**) WF-OCTA image showing the large-vessel choroidal layer in the same scan as **F**. (**I**) The *yellow highlight* indicates the presence of two PVVs around the optic disc in **G**. (**J1**) Horizontal WF-OCT image of **H** (*orange arrow*) corresponds to the 833th scan out of a total of 1280 WF-OCT scans, clearly demonstrating the exit of one PVV penetrating the sclera (*green arrowhead*) and leaving the eyeball. (**J2**) Horizontal WF-OCT image of **H** (*blue arrow*) corresponds to the 638th scan out of a total of 1280 WF-OCT scans, clearly demonstrating the exit of one PVV penetrating the sclera (*green arrowhead*) and leaving the eyeball. (**K–O2**) Two PVVs located around the optic disc in an eye with polypoidal choroidal vasculopathy. (**K**) Detection of two PVVs around the optic disc using the ICGA venous phase. (**L**) Detection of two PVVs around the optic disc using 24×20 mm en face WF-OCTA in the large-vessel choroidal layer. (**M**) WF-OCTA image showing the large-vessel choroidal layer in the same scan as **J**. (**N**) The *yellow highlight* indicates the presence of two PVVs around the optic disc in **K**. (**O1**) Horizontal WF-OCT image of **M** (*orange arrow*) corresponds to the 594th scan out of a total of 1280 WF-OCT scans, clearly demonstrating the exit of one PVV penetrating the sclera (*green arrowhead*) and leaving the eyeball. (**O2**) Horizontal WF-OCT image of **M** (*blue arrow*) corresponds to the 567th scan out of a total of 1280 WF-OCT scans, clearly illustrating the exit of another PVV penetrating the sclera (*green arrowhead*) and leaving the eyeball.

In our clinical work, we have noted that en face widefield optical coherence tomography angiography (WF-OCTA) effectively visualizes the PVVs in eyes with various diseases, as evident in the ICGA venous phase at 1 minute after dye injection (Fig. 1). This noninvasive imaging technique facilitates the detection of PVVs in healthy eyes, thereby obviating the necessity for invasive ICGA. Therefore, the purpose of this present study is to investigate the incidence and characteristics of PVVs in the eyes of healthy subjects, as well as their relationship with age and refractive status, using en face WF-OCTA.

METHODS

Subjects

This retrospective observational study received approval from the Institutional Review Board of the Zhongshan Ophthalmic Center at Sun Yat-Sen University (2023KYPJ116)

and adhered to the principles outlined in the Declaration of Helsinki. The study reviewed the data from a consecutive series of subjects with healthy eyes, including those with refractive errors. Subjects were excluded from the study if they exhibited poor fixation, had any opacity in the optical media that compromised image quality, presented a subfoveal choroidal thickness (SFCT) greater than 400 µm, or had any ocular diseases. A total of 510 eyes, with a best-corrected visual acuity (logarithm of the minimum angle of resolution) of 0, were included in the study. These eyes were derived from 255 healthy subjects who underwent examination at the Zhongshan Ophthalmic Center between March 2022 and March 2023.

The clinical variables analyzed in this study included age, gender, and refractive error. To confirm the absence of chorioretinal disorders, comprehensive ophthalmic assessments were performed using a slit-lamp biomicroscopy, indirect ophthalmoscope, WF-OCTA, en face WF-OCTA, and widefield optical coherence tomography (WF-OCT) imaging
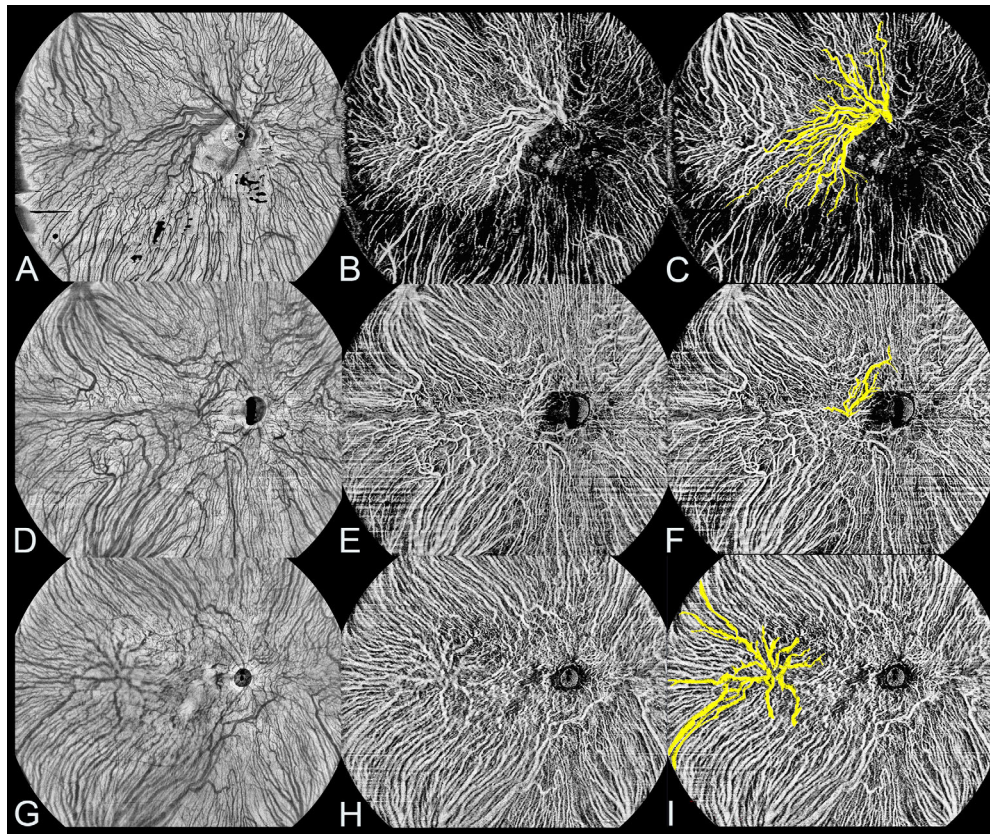
FIGURE 2. **WF-OCTA and en face WF-OCTA images of healthy eyes with different types of PVVs.** (**A–C**) PVV located around the optic disc in a healthy eye. (**A**) Detection of PVV around the optic disc using 24 × 20 mm en face WF-OCTA in the large-vessel choroidal layer. (**B**) WF-OCTA image showing the large-vessel choroidal layer in the same scan as **A**. (**C**) The *yellow highlight* indicates the presence of PVV around the optic disc in **B**. (**D–F**) PVV located at the macula area in another healthy eye. (**D**) Detection of PVV at the macula area using 24 × 20 mm en face WF-OCTA in the large-vessel choroidal layer. (**E**) WF-OCTA image showing the large-vessel choroidal layer in the same scan as **D**. (**F**) The *yellow highlight* indicates the presence of PVV at the macula area in **E**. (**G–I**) PVV located at other areas of the posterior pole in another healthy eye. (**G**) Detection of PVV at other areas of the posterior pole using 24 × 20 mm en face WF-OCTA in the large-vessel choroidal layer. (**H**) WF-OCTA image showing the large-vessel choroidal layer in the same scan as **G**. (**I**) The *yellow highlight* indicates the presence of PVV at other areas of the posterior pole in **H**.

with the TowardPi BMizar device (TowardPi Medical Technology, Beijing, China).

Widefield Swept-Source OCTA

In this study, participants were transitioned from a well-lit environment to a dark room in order to achieve optimal image quality with dilated pupils. The imaging procedures were conducted using the TowardPi BM400K BMizar, a widefield swept-source OCTA device manufactured by TowardPi Medical Technology (Beijing, China). This device operates at a high A-scan frequency of 400 kHz and utilizes a long wavelength of 1060 nm. WF-OCTA was captured in high-definition 24 × 20 mm (81 degrees × 68 degrees) sections centered on the fovea, with each image comprising 1280 line positions, 1536 A-scans for each line, and 2560 points on each A-scan. The scanning process was repeated twice to ensure data accuracy. Simultaneously, en face WF-OCTA and WF-OCT images were obtained. The OCTA images obtained in this study consist of three-dimensional data points, resulting in a substantial increase in data volume. The large-vessel choroidal layer refers to the slab located between 29 µm beneath the Bruch's membrane and the choroid-scleral interface (CSI). This region was automatically identified using the built-in software. To ensure the accuracy of the segmentation, we manually adjusted the layers in WF-OCT images when necessary. SFCT was measured using the tool provided by the built-in software.

Posterior Vortex Veins

The PVVs refer to the specific choroidal veins that serve as exits for the choroidal venous flow in the posterior pole region of the eye.[14] These veins can be classified into three types based on the location of the vortex vein exit from the eyes: those around the optic disc, those in the macula area, and those in other areas of the posterior pole (Fig. 2).

PVVs were identified in the large-vessel choroidal layer using en face WF-OCTA images. The exits of PVVs, where the vortex veins penetrate the sclera and exit the eyeball, were verified using WF-OCT imaging (see Fig. 1). The number, location, and area of each PVV were recorded, with the area measured using the software tool provided by the built-in software. All WF-OCTA, en face WF-OCTA, and WF-OCT images were independently evaluated by two trained investigators (authors G.H. and X.Z.). Any disagreements were resolved by a third retinal specialist (author F.W.) to reach a final determination.

In this study, all healthy eyes were categorized into different groups based on age and refractive status. The participants were divided into two age groups: the minors' group, comprising individuals aged 18 years or younger, and the adults' group, consisting of individuals older than 18 years. Regarding refractive status, the healthy eyes were further divided into three groups. The emmetropia group was defined as having a spherical equivalent between >−1.00 and ≤+1.00 diopters (D). The low and moderate myopia group was defined as having a spherical equivalent between >−6.00 and ≤−1.00 D.[16] Last, the high myopia group was defined as having a spherical equivalent of ≤−6.00 D.[17] These divisions allowed for a comprehensive analysis of the relationship among age, refractive error, and the incidence of PVVs in the study population.

Statistical Analysis

Statistical analysis was conducted using SPSS (version 26.0; SPSS, Inc., Chicago, IL, USA). Descriptive statistics were reported as the mean ± standard deviation (SD), median (interquartile range [IQR]), or as numbers (n) with percentages (%). The Fisher's exact test or Chi-square test was utilized to compare frequencies of categorical variables, such as sex, age status, and refractive status, as appropriate. For evaluating factors between two groups, the independent sample Student t-test or the Wilcoxon Mann-Whitney U test was applied, depending on the normal distribution of variables related to the clinical characteristics of eyes with or without PVVs. To assess factors among the three groups, the One-way ANOVA test or the Kruskal-Wallis H-test was used, depending on the normal distribution of variables related to PVVs. To address multiple testing among the 3 subgroups, Bonferroni and Tamhane test corrections were applied, adjusting the significance level to 0.0167. These corrections are crucial to minimize the chances of obtaining false positive results and maintain the integrity of the statis-

tical analysis. Logistic regression analysis was performed to determine the odds ratios (ORs) for the presence of PVVs. A P value of less than 0.05 was considered statistically significant.

RESULTS

A total of 510 eyes of 255 healthy subjects were included in this study. The age of the subjects ranged from 5 to 81 years (mean = 30.60 ± 21.12 years). The refractive error of the eyes ranged from −12.00 to +0.75 D (mean = −2.83 ± 3.10 D). Among the 510 eyes, PVVs were detected in 82 eyes (16.1%; Table 1).

A comparison of the clinical characteristics of eyes with and without PVVs is presented in Table 1. There was no significant difference in sex between the two groups. The mean age of subjects with PVVs (24.93 ± 19.52 years) was significantly lower than that of subjects without PVVs (31.69 ± 21.27 years; $P = 0.009$). The mean refractive error of eyes with PVVs (−3.84 ± 3.29 D) was slightly but significantly lower than that of eyes without PVVs (−2.64 ± 3.03 D, $P = 0.001$). The incidence of PVVs significantly increased with higher myopia status, with rates of 10.3%, 16.6%, and 26.4% in the emmetropia, low and moderate myopia, and high myopia groups, respectively ($P = 0.001$). The differences between emmetropia and high myopia ($P < 0.001$) and between low and moderate myopia and high myopia ($P = 0.043$) were significant. The mean SFCT of eyes with PVVs (212.39 ± 83.09 μm) was significantly thinner than that of eyes without PVVs (236.70 ± 76.81 μm, $P = 0.010$). No significant differences were observed in the incidence of PVVs between minor and adult subgroups in both the emmetropia and myopia groups (18.2% vs. 8.9%, $P = 0.121$ and 22.2% vs. 17.5%, $P = 0.312$; respectively; Supplementary Table S1). Additionally, in the logistic regression analysis, refractive status (OR = 1.45, 95% confidence interval [CI] = 1.02–2.06, $P = 0.038$) was the only significant predictor for the occurrence of PVVs (Table 2).

TABLE 1. Clinical Characteristics of the Healthy Subjects

Clinical Characteristics	All Subjects	Posterior Vortex Veins		P Value
		With	Without	
No. of eyes (%)	510	82/510 (16.1)	428/510 (83.9)	
Sex, no. (%)				0.826[*]
M	121 (47.4)	38/82 (46.3)	204/428 (47.7)	
F	134 (52.6)	44/82 (53.7)	224/428 (52.3)	
Age, y, mean ± SD (range)	30.60 ± 21.12 (5 ∼ 81)	24.93 ± 19.52 (5 ∼ 77)	31.69 ± 21.27 (5 ∼ 81)	0.009[†]
Age status, no. (%)				0.006[*]
Minors	204/510 (40.0)	44/204 (21.6)	160/204 (78.4)	
Adults	306/510 (60.0)	38/306 (18.4)	268/306 (87.6)	
Refractive error (D),	−2.83 ± 3.10	−3.84 ± 3.29	−2.64 ± 3.03	0.001[†]
mean ± SD (range)	(−12.00 to +0.75)	(−10.00 to +0.75)	(−12.00 to +0.75)	
Refractive status, no. (%)				0.001[*]
Emmetropia	213	22/213 (10.3)	191/213 (89.7)	
Low and moderate myopia	187	31/187 (16.6)	156/187 (83.4)	
High myopia	110	29/110 (26.4)	81/110 (73.6)	
SFCT (μm), mean ± SD (range)	232.79 ± 78.28 (51 ∼ 400)	212.39 ± 83.09 (62 ∼ 374)	236.70 ± 76.81 (51 ∼ 400)	0.010[‡]

D, diopter; SD, standard deviation; SFCT, subfoveal choroidal thickness.

Bonferroni-corrected post hoc analysis using Chi-square test ($P < 0.0167$ significant) comparing the three subgroups. Post hoc analysis for refractive status, <0.001# between around emmetropia and high myopia, and 0.043# between low and moderate myopia and high myopia.

[*] Fisher's exact test or Chi-square test.
[†] Wilcoxon Mann-Whitney U test.
[‡] Independent sample Student t-test.

TABLE 2. Odds Ratios for Logistic Regression Analysis of Posterior Vortex Vein Presence

|	Odds Ratio (95% Confidence Interval)	*P* Value
Age status	1.65 (0.99–2.75)	0.055
Sex	0.95 (0.59–1.54)	0.837
Refractive status	1.45 (1.02–2.06)	0.038
SFCT	0.99 (0.99–1.00)	0.099

SFCT, subfoveal choroidal thickness.

Further analysis of the eyes with PVVs revealed that 39.0% (32/82) had PVVs detected in only one eye of the subjects, whereas 61.0% (50/82) had PVVs detected in both eyes (Fig. 3). Among the eyes with PVVs, 97.6% (80/82) exhibited only one type, with 78.7% (63/80) located around the optic disc, 6.3% (5/80) in the macular area, and 15% (12/80) in other areas of the posterior pole. Only 2.4% (2/82) of the eyes had PVVs with 2 types (Fig. 4). The areas of PVVs ranged from 0.45 to 27.07 mm^2 (mean = 4.76 ± 5.36 mm^2). The number of PVVs per eye ranged from 1 to 6 (mean = 1.65 ± 1.05; Table 3).
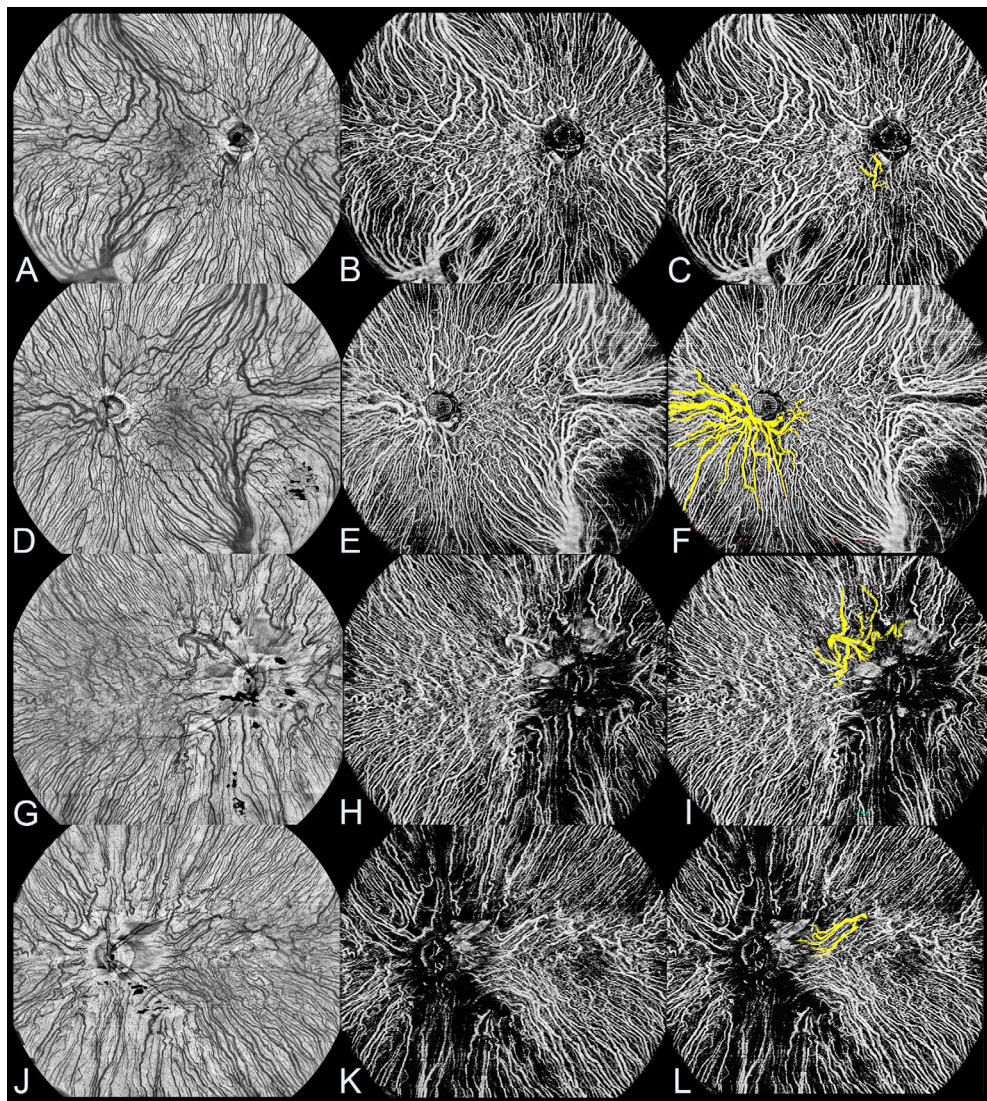
FIGURE 3. **WF-OCTA and en face WF-OCTA images of both eyes of healthy subjects with PVVs.** (**A–F**) PVV located around the optic disc in both eyes of a healthy subject. (**A–C**) PVV located around the optic disc in the right eye. (**A**) Detection of PVV around the optic disc in the right eye using 24 × 20 mm en face WF-OCTA in the large-vessel choroidal layer. (**B**) WF-OCTA image showing the large-vessel choroidal layer in the same scan as **A**. (**C**) The *yellow highlight* indicates the presence of PVV around the optic disc in **B**. (**D–F**) PVV located around the optic disc in the left eye. (**D**) Detection of PVV around the optic disc in the left eye using 24 × 20 mm en face WF-OCTA in the large-vessel choroidal layer. (**E**) WF-OCTA image showing the large-vessel choroidal layer in the same scan as **D**. (**F**) The *yellow highlight* indicates the presence of PVV around the optic disc in **E**. (**G–L**) PVV located at other areas of the posterior pole in both eyes of another healthy subject. (**G–I**) PVV located at other areas of the posterior pole in the right eye. (**G**) Detection of PVV at other areas of the posterior pole in the right eye using 24 × 20 mm en face WF-OCTA in the large-vessel choroidal layer. (**H**) WF-OCTA image showing the large-vessel choroidal layer in the same scan as **G**. (**I**) The *yellow highlight* indicating the presence of PVV at other areas of the posterior pole in **H**. (**J–L**) PVV located at other areas of the posterior pole in the left eye. (**J**) Detection of PVV at other areas of the posterior pole in the left eye using 24 × 20 mm en face WF-OCTA in the large-vessel choroidal layer. (**K**) WF-OCTA image showing the large-vessel choroidal layer in the same scan as **J**. (**L**) The *yellow highlight* indicates the presence of PVV at other areas of the posterior pole in **K**.
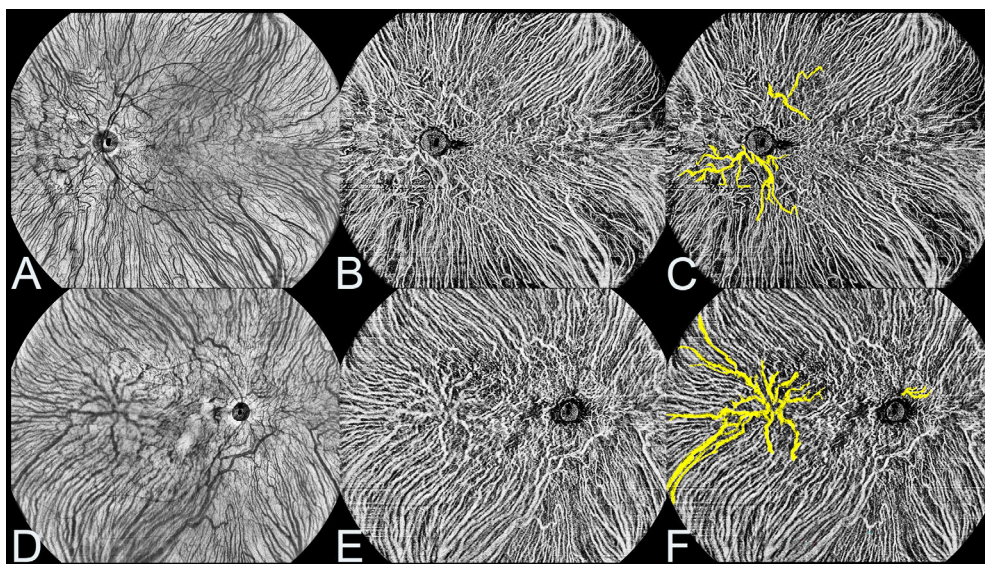
FIGURE 4. **WF-OCTA and en face WF-OCTA images of a single eye of healthy subjects with two types of PVVs.** (**A–C**) PVVs located around the optic disc and at other areas of the posterior pole in a single eye of a healthy subject. (**A**) Detection of two types of PVVs in the healthy eye using 24×20 mm en face WF-OCTA in the large-vessel choroidal layer. (**B**) WF-OCTA image showing the large-vessel choroidal layer in the same scan as **A**. (**C**) The *yellow highlight* indicating the presence of two types of PVVs in **B**. (**D–F**) PVVs located around the optic disc and at other areas of the posterior pole in a single eye of another healthy subject. (**D**) Detection of two types of PVVs in the healthy eye using 24×20 mm en face WF-OCTA in the large-vessel choroidal layer. (**E**) WF-OCTA image showing the large-vessel choroidal layer in the same scan as **D**. (**F**) The *yellow highlight* indicates the presence of two types of PVVs in **E**.

TABLE 3. Clinical Characteristics of Eyes With Posterior Vortex Veins

With Posterior Vortex Veins, No. (%)	Data
In eyes of all subjects	82
One type of posterior vortex vein	80/82 (97.6)
Around optic disc	63/80 (78.7)
Macular area	5/80 (6.3)
Other area	12/80 (15.0)
Two types of posterior vortex veins	2/82 (2.4)
Only in one eye of subjects	32/82 (39.0)
One type of posterior vortex vein	31/32 (96.9)
Around optic disc	23/31 (74.2)
Macular area	2/31 (6.5)
Other area	6/31 (19.3)
Two types of posterior vortex veins	1/32 (3.1)
In both eyes of subjects	50/82 (61.0)
One type of posterior vortex vein	49/50 (98.0)
Around optic disc	40/49 (81.6)
Macular area	3/49 (6.1)
Other area	6/49 (12.2)
Two types of posterior vortex veins	1/50 (2.0)
Posterior vortex vein area (mm^2)	
Median (IQR)	2.87 (3.85)
Mean $\pm$ SD (range)	4.76 ± 5.36 (0.45 ~ 27.07)
Posterior vortex veins per eye (no.)	
Median (IQR)	1.00 (1)
Mean $\pm$ SD (range)	1.65 ± 1.05 (1 ~ 6)

IQR, interquartile range; SD, standard deviation.

The clinical characteristics of eyes with PVVs in different refractive status are summarized in Table 4. The mean SFCT differed significantly among the refractive status groups of eyes with PVVs (230.91 ± 83.31 μm for emmetropia, 240.35 ± 75.40 μm for low and moderate myopia, and 168.45 ± 74.45 μm for high myopia, $P = 0.001$). The differences in SFCT between emmetropia and high myopia ($P = 0.016$), as well as between low and moderate myopia and high myopia ($P = 0.002$), were statistically significant. The presence of PVVs, whether in one eye or both eyes, did not differ significantly among the refractive status groups ($P = 0.291$). However, there was a significant difference in the location of unilateral PVVs among the refractive status groups ($P = 0.035$). Specifically, the difference between emmetropia and low and moderate myopia in terms of PVVs around optic disc was significant ($P = 0.006$). The mean area of PVVs and mean number of PVVs per eye did not differ significantly among the refractive status groups ($P = 0.219$ and $P = 0.776$, respectively).

The clinical characteristics of the eyes with different types of PVVs are summarized in Table 5. The majority of PVVs were located around the optic disc (78%, 64/82), whereas the rest were distributed across other regions of the posterior pole (15.9%, 13/82) and the macular area (6.1%, 5/82). Significant differences were observed in age and SFCT between different types of PVVs ($P = 0.008$ and $P = 0.012$, respectively). The maximum number of PVVs observed per eye was six around the optic disc (Fig. 5), with up to three observed in the macular area and up to two in other areas of the posterior pole. However, there were no significant differences in the number of PVVs per eye or the area of PVVs among the three locations of the PVV exit ($P = 0.097$ and $P = 0.054$, respectively).

DISCUSSION

In this study, we investigate the incidence of PVV in the eyes of healthy subjects and explored their relationship with age and refractive status. To the best of our knowledge, this study is the first to observe PVVs in healthy eyes. Our findings revealed that PVVs were present in 16.1%

TABLE 4. Clinical Characteristics of Eyes in Different Refractive Status With Posterior Vortex Veins

Clinical Characteristic	Myopia With Posterior Vortex Veins			P Value
	Emmetropia	Low and Moderate Myopia	High Myopia	
No. of eyes	22	31	29	
Sex, no. (%)				
M	7/22 (31.8)	13/31 (41.9)	18 (62.1)	
F	15/22 (68.2)	18/31 (58.1)	11 (37.9)	
Age, y, mean ± SD (range)	41.77 ± 24.65 (8 ∼ 77)	14.71 ± 8.30 (5 ∼ 43)	23.07 ± 15.17 (5 ∼ 65)	
Refractive error (D), mean ± SD (range)	0.00 ± 0.23 (−0.75 to +0.75)	−3.00 ± 1.44 (−5.75 to −1.00)	−7.66 ± 1.26 (−10.00 to −6.00)	
SFCT (μm), mean ± SD (range)	230.91 ± 83.31 (79 ∼ 361)	240.35 ± 75.40 (91 ∼ 360)	168.45 ± 74.45 (62 ∼ 374)	0.001[¶]
Posterior vortex veins, no. (%)				0.291[*]
Only in one eye of subjects	10/22 (45.5)	14/31 (45.2)	8/29 (27.6)	0.035[*]
Around optic disc	4/10 (40.0)	13/14 (92.9)	6/8 (75.0)	
Macular area	2/10 (20.0)	0	0	
Other area	4/10 (40.0)	1/14 (7.1)	2/8 (25.0)	
In both eyes of subjects	12/22 (54.5)	17/31 (54.8)	21/29 (72.4)	0.214[*]
Around optic disc	10/12 (83.3)	13/17 (76.5)	18/21 (85.7)	
Macular area	2/12 (16.7)	1/17 (5.9)	0	
Other area	0	3/17 (17.6)	3/21 (14.3)	
Posterior vortex vein area (mm^2)				0.219[§]
Median (IQR)	3.12 (6.79)	2.47 (2.64)	3.28 (5.06)	
Mean ± SD (range)	6.04 ± 6.86 (0.54 ∼ 21.82)	3.14 ± 0.52 (0.57 ∼ 10.11)	5.52 ± 6.02 (0.45 ∼ 27.07)	
Posterior vortex veins per eye (no.)				0.776[§]
Median (IQR)	1.00 (1)	1.00 (1)	1.00 (1)	
Mean ± SD (range)	1.77 ± 1.19 (1 ∼ 6)	1.58 ± 1.06 (1 ∼ 6)	1.62 ± 0.94 (1 ∼ 5)	

D, diopter; IQR, interquartile range; SD, standard deviation; SFCT, subfoveal choroidal thickness.

Bonferroni-corrected post hoc analysis using One-way ANOVA test ($P < 0.0167$ significant) comparing the three subgroups. Post hoc analysis for SFCT, 0.016# between around emmetropia and high myopia, and 0.002# between low and moderate myopia and high myopia.

Bonferroni-corrected post hoc analysis using Chi-square ($P < 0.0167$ significant) comparing the three subgroups. Post hoc analysis for around optic disc in one posterior vortex vein, 0.006# between emmetropia and low and moderate myopia.

[*] Fisher's exact test or Chi-square test.
[¶] One-way ANOVA test.
[§] Kruskal-Wallis H-test.

TABLE 5. Clinical Characteristics of the Eyes With Different Types of Posterior Vortex Veins

Clinical Characteristic	Location of the Posterior Vortex Vein Exit			P Value
	Around Optic Disc	Macular Area	Other Area	
Posterior vortex veins (eyes), no. (%)	64/82 (78.0)	5/82 (6.1)	13/82 (15.9)	
Sex, no. (%)				0.470[*]
M	31/64 (48.4)	1/5 (20.0)	6/13 (46.2)	
F	33/64 (51.6)	4/5 (80.0)	7/13 (53.8)	
Age, y, mean ± SD (range)	19.94 ± 13.62 (5 ∼ 74)	53.00 ± 22.49 (13 ∼ 67)	38.69 ± 27.59 (8 ∼ 77)	0.008[§]
Refractive error (D), mean ± SD (range)	0.00 ± 0.23 (−0.75 to +0.75)	−1.00 ± 2.24 (−5.00 to 0.00)	−4.21 ± 4.05 (−10.00 to 0.00)	0.097[§]
SFCT (μm), mean ± SD (range)	225.06 ± 78.76 (68 ∼ 374)	165.80 ± 32.48 (124 ∼ 210)	167.92 ± 98.93 (62 ∼ 344)	0.012[¶]
Posterior vortex vein area (mm^2)				0.054[§]
Median (IQR)	2.51 (3.52)	4.44 (12.85)	4.57 (5.61)	
Mean ± SD (range)	4.19 ± 5.05 (0.45 ∼ 27.07)	7.47 ± 7.14 (1.56 ∼ 18.36)	6.54 ± 5.88 (1.79 ∼ 21.82)	
Posterior vortex veins per eye (no.)				0.097[§]
Median (IQR)	1.00 (1)	1.00 (2)	1.00 (0)	
Mean ± SD (range)	1.75 ± 1.13 (1 ∼ 6)	1.6 ± 0.89 (1 ∼ 3)	1.15 ± 0.38 (1 ∼ 2)	

D, diopter; IQR, interquartile range; SD, standard deviation; SFCT, subfoveal choroidal thickness.

Tamhane test post hoc analysis using One-way ANOVA test ($P < 0.0167$ significant) comparing the three subgroups. Post hoc analysis for SFCT, 0.027# between around the optic disc and macular area.

Bonferroni-corrected post hoc analysis using Kruskal-Wallis H-test ($P < 0.0167$ significant) comparing the three subgroups. Post hoc analysis for age, 0.027# between around the optic disc and macular area.

[*] Fisher's exact test or Chi-square test.
[¶] One-way ANOVA test.
[§] Kruskal-Wallis H-test.

(82/510) of healthy eyes. The incidence of PVVs increased gradually with different refractive statuses, with rates of 10.3% (22/213), 16.6% (31/187), and 26.4% (29/110) in the emmetropia, low and moderate myopia, and high myopia groups, respectively. Surprisingly, the incidence of PVVs did not differ significantly between different age groups. Refrac-
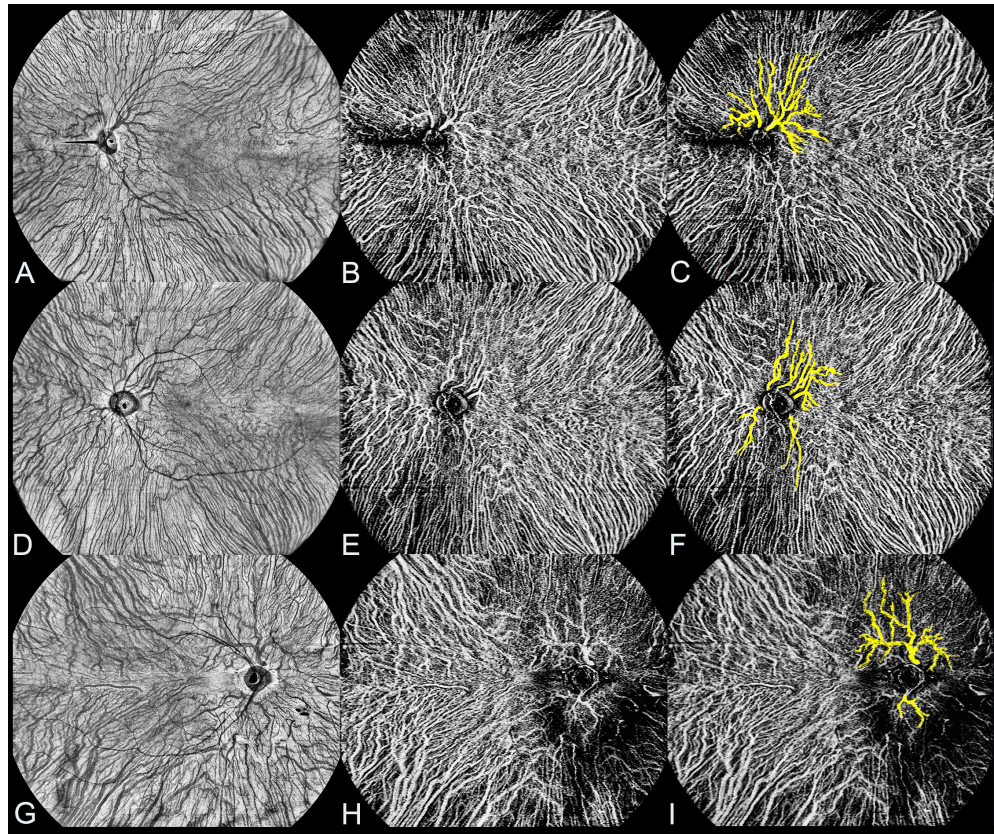
FIGURE 5. **WF-OCTA and en face WF-OCTA images of a single eye of healthy subjects with multiple PVVs.** (**A–C**) Two PVVs located around the optic disc in a single eye of a healthy subject. (**A**) Detection of two PVVs around the optic disc in the healthy eye using 24 × 20 mm en face WF-OCTA in the large-vessel choroidal layer. (**B**) WF-OCTA image showing the large-vessel choroidal layer in the same scan as **A**. (**C**) The *yellow highlight* indicates the presence of two PVVs around the optic disc in **B**. (**D–F**) Six PVVs located around the optic disc in a single eye of another healthy subject. (**D**) Detection of six PVVs around the optic disc in the healthy eye using 24 × 20 mm en face WF-OCTA in the large-vessel choroidal layer. (**E**) WF-OCTA image showing the large-vessel choroidal layer in the same scan as **D**. (**F**) The *yellow highlight* indicates the presence of six PVVs around the optic disc in **E**. (**G–I**) Two PVVs located around the optic disc in a single healthy eye of another healthy subject. (**G**) Detection of two PVVs around the optic disc in the healthy eye using 24 × 20 mm en face WF-OCTA in the large-vessel choroidal layer. (**H**) WF-OCTA image showing the large-vessel choroidal layer in the same scan as **G**. (**I**) The *yellow highlight* indicates the presence of two PVVs around the optic disc in **H**.

tive status was the only significant predictor for the occur of PVVs.

Traditionally, it was widely believed that the ampullae of the vortex veins located at the equator are equally distributed in four quadrants, forming a "watershed zone" between them. However, a few reports in the literature have described the presence of ampullae of the vortex veins at the macular region associated with various diseases, such as congenital glaucoma in a patient with trisomy 13 syndrome, diabetes mellitus, oculocutaneous albinism, and focal choroidal excavation.[7–10] Additionally, PVVs have been found to be more common in eyes with high myopia.[11–15] In our study, we made the significant observation that vortex veins can also be detected in the posterior pole of healthy eyes, specifically in emmetropic eyes, challenging the previous notion that ampullae of the vortex veins are primarily located at the equator. This finding provides new insights into the distribution of vortex veins within the eyes, particularly in healthy eyes.

More interestingly, the incidence of PVVs was essentially the same in different age status between the minors' and adults' groups. Of note, the youngest age included in this study was 5 years, and the youngest subject with

emmetropic eyes was 8 years. Although Table 1 shows that the presence of PVVs was correlated with age, no relationship was found with age status in further grouping and logistic regression. Actually, this is owing to the retrospective and hospital-based nature of this study, there are more patients with myopia in the minors' group. In addition, our findings revealed that in healthy subjects, 61% (50 out of 82) of the identified PVVs were present in both eyes, although the simultaneous presence of these veins did not show significant variation across the three different refractive status groups. Notably, two subjects had two different types of exit locations for the vortex veins in the posterior pole region, a finding that has not been previously reported. Therefore, we reasonably hypothesize that the exits of vortex veins could be present innately in the posterior pole, although the majority of them are observed to exit at the equator. These novel findings expand our understanding of the vortex vein system and its distribution within the eyes.

Our study further revealed that 26.4% (29/110) of eyes in the high myopia group exhibited PVV, which is consistent with previous reports by Moriyama et al. (26%, 80/302) and Ohno-Matsui et al. (24%, 61/255).[13,15] Interestingly, we observed a gradual increase in the incidence of PVVs across

different refractive statuses, including emmetropia, low and moderate myopia, and high myopia groups. Several factors may contribute to these findings. First, numerous clinical studies consistently demonstrate that choroidal thickness decreases with longer axial length (AL) and lower refractive error.[18,19] Refractive error shows a strong inverse correlation with the AL of the eyes.[20] Myopia, particularly high myopia, is associated with reduced choroidal blood flow.[21] As the AL increases and the eye globe expands, the choroid tends to become thinner, leading to a reduced relative volume of choroidal veins. Consequently, this compression between the sclera and the retinal pigment epithelium (RPE) impedes venous reflux and hampers blood flow from the posterior pole into the vortex veins, ultimately resulting in reduced venous drainage. Second, recent findings by Xie et al. have demonstrated the presence of macular dilated choroidal veins (DCVs), some of which are PVVs in myopic macular neovascularization (MNV).[22] They observed a higher recurrence rate of MNV in eyes with DCVs compared to those without DCVs. These findings suggest that decreased choroidal perfusion and subsequent expression of ischemia-induced growth factors might contribute to the development of MNV.[23] Third, Moriyama et al. reported cases of posterior vortex veins enlarging over time during long-term follow-up.[14] This indicates that there might be dynamic changes in the choroidal venous system associated with high myopia. Last, Moriyama et al. discovered a significant association between PVVs and posterior staphyloma. Eyes with PVVs were more frequently associated with staphyloma compared to those without PVVs, as observed using conventional ICGA.[15] They reported that the choroidal venous flow ceased at the border of the posterior staphyloma and flowed sluggishly toward the periphery. In two cases, they observed secondary occlusion of the choroidal venous flow at the staphyloma border, resulting in alterations in the course of choroidal venous flow and the formation of collateral channels beyond the less steep edge of the staphyloma.[14] These findings suggest that choroidal ischemia in highly myopic eyes, especially those with staphyloma, could lead to remodeling of choroidal venous reflux and potentially give rise to the emergence of PVVs.

Interestingly, our study revealed a predominant presence of PVVs around the optic disc, followed by the other areas of the posterior pole and macular area. The optic disc region exhibited the highest maximum number of PVVs, suggesting a potential role of the optic disc in the emergence or maintenance of PVVs. The optic nerve head (ONH) consists of the ONH canal and the parapapillary region, with the ONH canal wall comprising three layers: the inner layer being the Bruch's membrane opening (BMO), the middle layer being the choroidal opening, and the outer layer being the lamina cribrosa. These three layers are aligned and form a mostly perpendicular angle with the sclera at birth.[24] In cases of axial elongation, the BMO undergoes enlargement, resulting in the retraction of the intrapapillary overhanging Bruch's membrane.[25] This leads to the development of a circular gamma zone and delta zone, with the arterial circle of Zinn-Haller marking the border between them.[24] This arterial circle serves to nourish the ONH, including the lamina cribrosa.[26,27] As the delta zone elongates, the distance between the arterial circle and the lamina cribrosa increases.[24,26] This elongation-induced increase in distance, combined with choroidal ischemia, may contribute to the higher prevalence of PVVs in individuals with high myopia. These findings suggest a plausible association among axial elongation, choroidal ischemia, and the presence of PVVs.

It is worth noting that our study had several limitations. First, the retrospective cross-sectional design limits our ability to establish causality and draw definitive conclusions. Future longitudinal studies are necessary to further explore the relationship between PVVs and age or refractive status. Second, we utilized noninvasive en face WF-OCTA imaging instead of traditional ICGA examination, which may have limitations in accurately visualizing choroidal veins. Third, due to the retrospective nature of the study and the patient population at the hospital, there was a higher proportion of patients with myopia in the minors' group, which might have influenced the results. However, we conducted further subgroup analyses and logistic regression to mitigate this potential bias. Additionally, the lack of complete axial length data for all subjects is another limitation. Despite these limitations, our study provides novel insights into the distribution and characteristics of PVVs in a relatively large sample of healthy individuals who did not undergo invasive ICGA examination.

In conclusion, our study demonstrated the presence and features of PVVs in healthy eyes using en face WF-OCTA imaging. We also observed the congenital appearance of PVVs in healthy eyes and identified refractive status as a key factor influencing their occurrence. These findings contribute to our understanding of the vortex vein system and its distribution within the eyes.

References

1. Hayreh SS, Hayreh SB. Uveal vascular bed in health and disease: uveal vascular bed anatomy. Paper 1 of 2. Eye 2023. Available at: https://www.nature.com/articles/s41433-023-02416-z. Accessed May 22, 2023.

2. Nickla DL, Wallman J. The multifunctional choroid. *Prog Retinal Eye Res*. 2010;29:144–168.

3. Yu D-Y, Yu PK, Cringle SJ, et al. Functional and morphological characteristics of the retinal and choroidal vasculature. *Prog Retinal Eye Res*. 2014;40:53–93.

4. Verma A, Maram J, Alagorie AR, et al. Distribution and location of vortex vein ampullae in healthy human eyes as assessed by ultra-widefield indocyanine green angiography. *Ophthalmol Retina*. 2020;4:530–534.

5. Lim MC, Bateman JB, Glasgow BJ. Vortex vein exit sites. *Ophthalmology*. 1995;102:942–946.

6. Rutnin U. Fundus appearance in normal eyes. I. The choroid. *Am J Ophthalmol*. 1967;64:821–839.

7. Lichter PR, Schmickel RD. Posterior vortex vein and congenital glaucoma in a patient with trisomy 13 syndrome. *Am J Ophthalmol*. 1975;80:939–942.

8. Sekimoto M, Hayasaka S, Watanabe M, Setogawa T. Vortex veins in the macula. *Ophthalmologica*. 1988;197:34–35.

9. Lobo S, Pradeep N, Rajendran A. Bilateral macular vortex veins in oculocutaneous albinism. *JAMA Ophthalmol*. 2022;140:e223926.

10. He G, Zhang X, Wen F. Subfoveal focal choroidal excavation with macular vortex vein. *Ophthalmol Retina*. 2024; 8:9.

11. Ohno-Matsui K, Morishima N, Teramatsu T, Tokoro T, Nakagawa T. The long-term follow-up of a highly myopic patient with a macular vortex vein. *Acta Ophthalmol Scand*. 1997;75:329–332.

12. Kaplan RI, Walsh JB, Rosen RB, Gupta M. Macular vortex vein in a highly myopic eye imaged by optical coherence tomography angiography. *Retin Cases Brief Rep*. 2021;15:431–435.

13. Ohno-Matsui K, Morishima N, Ito M, et al. Posterior routes of choroidal blood outflow in high myopia. *Retina*. 1996;16:419–425.

14. Moriyama M, Ohno-Matsui K, Futagami S, et al. Morphology and long-term changes of choroidal vascular structure in highly myopic eyes with and without posterior staphyloma. *Ophthalmology*. 2007;114:1755–1762.e1.

15. Moriyama M, Cao K, Ogata S, Ohno-Matsui K. Detection of posterior vortex veins in eyes with pathologic myopia by ultra-widefield indocyanine green angiography. *Br J Ophthalmol*. 2017;101:1179–1184.

16. Chua W-H, Balakrishnan V, Chan Y-H, et al. Atropine for the treatment of childhood myopia. *Ophthalmology*. 2006;113:2285–2291.

17. Ruiz-Medrano J, Montero JA, Flores-Moreno I, et al. Myopic maculopathy: current status and proposal for a new classification and grading system (ATN). *Prog Retin Eye Res*. 2019;69:80–115.

18. Hoseini-Yazdi H, Vincent SJ, Collins MJ, et al. Wide-field choroidal thickness in myopes and emmetropes. *Sci Rep*. 2019;9:3474.

19. Jonas JB, Jonas RA, Bikbov MM, et al. Myopia: histology, clinical features, and potential implications for the etiology of axial elongation. *Prog Retinal Eye Res*. 2023;96: 101156.

20. Foster PJ, Broadway DC, Hayat S, et al. Refractive error, axial length and anterior chamber depth of the eye in British adults: the EPIC-Norfolk Eye Study. *Br J Ophthalmol*. 2010;94:827–830.

21. Liu Y, Wang L, Xu Y, et al. The influence of the choroid on the onset and development of myopia: from perspectives of choroidal thickness and blood flow. *Acta Ophthalmol*. 2021;99:730–738.

22. Xie S, Du R, Fang Y, et al. Dilated choroidal veins and their role in recurrences of myopic macular neovascularisations. *Br J Ophthalmol*. 2022;106:1429–1435.

23. Wakabayashi T, Ikuno Y. Choroidal filling delay in choroidal neovascularisation due to pathological myopia. *Br J Ophthalmol*. 2010;94:611–615.

24. Jonas JB, Spaide RF, Ostrin LA, et al. IMI—nonpathological human ocular tissue changes with axial myopia. *Invest Ophthalmol Vis Sci*. 2023;64:5.

25. Zhang Q, Xu L, Wei WB, et al. Size and shape of Bruch's membrane opening in relationship to axial length, gamma zone, and macular Bruch's membrane defects. *Invest Ophthalmol Vis Sci*. 2019;60:2591.

26. Wang YX, Panda-Jonas S, Jonas JB. Optic nerve head anatomy in myopia and glaucoma, including parapapillary zones alpha, beta, gamma and delta: histology and clinical features. *Prog Retinal Eye Res*. 2021;83:100933.

27. Ishida T, Jonas JB, Ishii M, et al. Peripapillary arterial ring of Zinn-Haller in highly myopic eyes as detected by optical coherence tomography angiography. *Retina*. 2017;37:299–304.